GROWTH IN COMPLEX EXPONENTIAL DYNAMICS

M. ROMERA, G. PASTOR[†], G. ALVAREZ and F. MONTOYA

Instituto de Física Aplicada, Consejo Superior de Investigaciones Científicas, Serrano 144, 28006 Madrid, Spain
e-mail: gerardo@iec.csic.es

Abstract— Both the computer drawing of the complement of the Mandelbrot-like set of a one-parameter dependent complex exponential family of maps and the computer drawing of the Julia sets of the maps of this family, grow with the maximal number of iterations we choose. Some graphic examples of this growth, which evoke the image of a garden, are shown here.

1. INTRODUCTION

During the period 1918-20 the field of complex analytic dynamics showed a vigorous growth when Julia [1] and Fatou [2] became interested in the behavior of complex functions under iteration. Sometimes the results of iteration were quite tame or stable; at other times these iterations behaved in a dramatically different fashion —what we now call chaotic behavior (see a historical overview of complex dynamics in [3]).

In 1980, Mandelbrot [4] used computer graphics to explore complex dynamics. His discovery of the Mandelbrot set [4, 5] prompted many mathematicians as Douady and Hubbard [6], Peitgen and Richter [7], Branner [8], and Milnor [9] to reinvestigate the field of complex dynamics.

1.1. *The Julia set of a complex map*

Let $z_{n+1} = f_\lambda(z_n)$ be a family of complex maps, where λ is a complex parameter. Let us consider a map of this family corresponding to a given parameter value. As is well known [8], the dynamical plane for f_λ decomposes into two disjoint subsets: the set of seeds (initial values) with bounded orbit, and the set of seeds with unbounded orbit. We denote by

$$K_\lambda = \left\{ z \in \mathbf{C} \middle| f_\lambda^n(z) \not\to \infty \text{ when } n \to \infty \right\}, \qquad (1)$$

the set of seeds with bounded orbit. The dynamical plane can also be decomposed into two other disjoint subsets: the stable set on which the dynamics are tame (bounded or unbounded orbits), and the Julia set J_λ on which the dynamics are chaotic [8]. The set K_λ is also called the filled-in Julia set, since J_λ is the set of boundary points of K_λ.

In practice, it is not possible to iterate a map an infinite number of times but only a finite one. We must thus choose an integer *N*, the maximal number of iterations the computer will be asked to do. Then, the computer drawing of a Julia set will really be an approximation of the Julia set.

1.2. *The Mandelbrot-like set of a family of complex maps*

For the quadratic family of complex maps $z_{n+1} = z_n^2 + c$, Douady and Hubbard [6] have shown that K_c is a connected set if $0 \in K_c$ and a Cantor set otherwise. For this family of maps, the set of values of c for which K_c is connected was initially called the M set [5, 6] and latter the Mandelbrot set [7,10]. As is well known, the Mandelbrot set can also be defined as the set of values of c for which, beginning with the initial value $z_0 = 0$, the sequence z_n remains bounded.

Starting from the work of Mandelbrot [11], a family of maps can be studied from a graphical point of view. A transformation becomes easier to study when one has a concrete visual feeling for its action [5]. We have previously used this technique in the study of the ordering of periodic orbits of the one-parameter family of real quadratic maps $x_{n+1} = x_n^2 + c$ [12], using the drawing of the Mandelbrot set antenna.

In general, the Mandelbrot-like set of a family of complex maps $z_{n+1} = f_\lambda(z_n)$ for the initial value z_0 (usually the one corresponding to the critical point of the family of maps) is defined as the set of $\lambda \in \mathbf{C}$ for which the *n*-th iteration of the function $f_\lambda^n(z_0)$ does not tend to ∞ as *n* tends to ∞

$$\mathrm{M} = \left\{ \lambda \in \mathbf{C} \middle| f_\lambda^n(z_0) \not\to \infty \text{ when } n \to \infty \right\}. \qquad (2)$$

As we said in §1.1, it is not possible to iterate a map an infinite number of times but only a finite one. We must thus choose an integer *N*, the maximal number of iterations the computer will be asked to do. Then, the computer drawing of a Mandelbrot-like set will really be an approximation of the Mandelbrot-like set.

2. COMPLEX EXPONENTIAL DYNAMICS

Iterates of the complex exponential map $z_{n+1} = e^{z_n}$ ($z \in \mathbf{C}$) were studied for the first time by Misiurewicz [13] from a mathematical point of view. Latter, Baker and Rippon [14] studied the iteration of the family of complex exponential maps $z_{n+1} = e^{\lambda z_n}$ and, independently, Devaney [15] studied the iteration of the family of complex exponential maps $z_{n+1} = \lambda e^{z_n}$. In the last two cases, the two families of maps were also studied from a mathematical point of view, but the Mandelbrot-like set of each one of them was also drawn. It is easy to show that the Mandelbrot-like set of $z_{n+1} = e^{\lambda z_n}$ and the Mandelbrot-like set of $z_{n+1} = \lambda e^{z_n}$ are the same. For this reason, we call this picture the Baker-Rippon-Devaney (BRD) set [16].

We shall consider three families of complex exponential maps:

$$E_{1\lambda}(z) = \lambda e^z \,, \tag{3}$$

$$E_{2\lambda}(z) = e^{z^2+\lambda} \,, \tag{4}$$

and

$$E_{3\lambda}(z) = e^{z/\lambda} \,. \tag{5}$$

When λ is a real parameter, the Julia sets of Eq. (3) have the interesting property, found out by Devaney, that they "may explode" as the parameter λ is varied [17, 18]. One such explosion occurs when $\lambda = 1/e$. For λ less than this critical value, Devaney showed that the Julia set occupies a relatively small, nowhere dense subset of the right half plane; but when $\lambda > 1/e$ the Julia set covers the whole plane. Just for $\lambda = 1/e$ the "explosion" occurs.

Recently we have studied the families of complex exponential maps of Eqs. (3), (4) and (5) from a graphical point of view, and we have shown that both the computer drawing of the complement of the Mandelbrot-like set of each one of them and the computer drawing of the Julia sets of the maps of these families, "grow" with N [19]. In the case of colored graphics, the "growth" evokes the image of a blossoming garden. This work is an extended version of our previous work [19].

3. DRAWING COMPLEX EXPONENTIAL DYNAMICS

3.1 *Escape criterion*

According to [14], it may be noted that the iteration of a family of complex exponential maps has many parallels with that of Douady and Hubbard [6], who examine the iteration of the family of complex quadratic maps $f_c(z) = z^2 + c$. But there is a fundamental difference between the iteration of a family of complex exponential maps and the iteration of a family of complex quadratic maps: no longer do we have an exact escape criterion for the family of complex exponential maps [20].

When we iterate the quadratic map, the well known escape criterion is "the orbit escapes when $|z| > 2$" [5]. So, if we have $|z| > 2$ for some *n*, then $f_c^n(0) \to \infty$ when $n \to \infty$. Nevertheless, there was no escape criterion for exponential maps until Devaney [20] introduced the following approximate one: "the orbit escapes if the real part of z ($\operatorname{Re} z$) exceeds bound $B = 50$."

The initial value z_0 is chosen to be the critical point of the family of maps, i.e. $z_0 = 0$ for the family of Eq. (4). But the families of Eqs. (3) and (5) have no critical point, and the role of the critical value is played by 0. Technically, 0 is an asymptotic value [21]. According to this, we iterate all the families of maps of Eqs. (3), (4) and (5) from the initial value $z_0 = 0$.

3. 2. *Computer drawing algorithm*

The computer program to iterate a complex map can use a complex or real library. When it is possible to write the program using only real functions, it is well known that the execution time can be decreased. This happens in the case of the iteration of Eqs. (3), (4) and (5), where we can use Euler's formula. For example, let us consider the iteration of Eq. (3). Given the real and imaginary parts of both λ and z_n ($\lambda = \alpha + \beta i$, $z_n = x_n + y_n i$), the real and imaginary parts of z_{n+1} are

$$\begin{aligned} \operatorname{Re} z_{n+1} &= x_{n+1} = e^{x_n}(\alpha \cos y_n - \beta \sin y_n) \,, \\ \operatorname{Im} z_{n+1} &= y_{n+1} = e^{x_n}(\alpha \operatorname{sen} y_n + \beta \cos y_n) \,. \end{aligned} \tag{6}$$

In this work, the pictures are black and white or colored ones. In the first case, a point of the picture is black if the corresponding orbit does not escape to ∞, and it is white if the orbit escape to ∞. In the last case, according to Devaney [17], we color such a point with a scheme that assigns the color depending on the number of iterations that have occurred before escape (if the orbit does not escape to ∞ the color of the point is black). The algorithms that we have used for drawing the black and white pictures of this work, for the family of Eq. (3), are given in the appendices. We show the algorithm to draw the BRD set in Appendix A, and we show the algorithm to draw a Julia set in Appendix B.

4. THE BRD SET

As we said in §2, we call the BRD set the Mandelbrot-like set of the family of maps $E_{1\lambda}(z) = \lambda e^z$. In Fig. 1 we can see the BRD set which extends from $-\infty$ to ∞ for both real and imaginary values. The real axis is an axis of symmetry, and the figure is almost periodic with period 2π along the imaginary axis. This BRD set has been obtained by means of the algorithm of Appendix A. Each black motif, $C_p = \{\lambda \in \mathbf{C} | E_{1\lambda}$ has an attracting periodic orbit of period - $p\}$, is marked by means of a white number in the figure. So, the period-1 component C_1 is bounded by a cardioid curve (with its cusp at $\lambda = 1/e$

and its low curvature point at $\lambda = -e$). For each integer $p \geq 2$ and for each primitive *p*-th root of unity η there is a domain C_p , which lies outside C_1 but is tangent to C_1 at $\lambda = \eta e^{-\eta}$ (a similar situation occurs in the well known Mandelbrot set, where there is a period-1 domain bounded by a cardioid and there are period-*p* disks connected to it through only one point). Devaney called such a domain a "tongue" [15].

4.1. *Tongues*

In Fig. 1 we can see many tongues in the BRD set as, for example, tongues of periods 3, 5, 7, 9 and 11 attached to the period-1 domain bounded by the cardioid. A tongue is simply connected and extends to infinity [15]. The bigger one, the period-2 tongue, is a domain tangent to C_1 at $\lambda = -e$ and is lying on the left half-plane. This tongue is unique since it is the only period different from one for which there is a single component (all the other periods have infinitely many components), and it has infinitely many cusp-like points as well as additional higher period tongues emanating at roots of unity [15]. Each one of the tongues of BRD set has a tail which extents as far as ∞ (in Fig. 1 tongues are not unbounded but amputated for the reasons we shall see afterwards). Each tongue has an infinity of smaller tongues attached to it, and so on. The BRD set is a fractal.

However, there are tongues that are not connected to the period-1 component bounded by the cardioid. In the same way as the Mandelbrot set hyperbolic components are classified into cardioids and disks, we classify the tongues of the BRD set into cardioid tongues (if they are not connected to the period-1 component) and into disk tongues (if they are connected to the period-1 component) [16]. For example, in Fig. 1 we can see two different period-4 tongues: a disk tongue at $1+0.4\,i$, and a cardioid tongue at $0.2+3.8\,i$.

4.2. *Fingers*

Separating the tongues of the BRD set are the white motifs that we call "fingers". The word "finger" was introduced by Devaney and Durkin [18] when they described the geometry of the Julia set of a map of the family $E_{1\lambda}(z) = \lambda e^{z}$. In Fig. 1 we can see many fingers; each one of them is marked by means of an index [16], a black number. The index of a finger is the same as the period of the tongues that it separates. The fingers are artifacts of the limitations of the computer and do not really exist: they indicate parameter values where the orbit escapes beyond a certain bound in the right half-plane. On account of using the approximate escape criterion, fingers cover the thin part of the tongue tails.

Due to computer limitations, we must use a relatively low bound *B*. The reason for this choice of a low bound is the problems encountered when computing e^{B} [21] (a discussion of the accuracy and pitfalls of the approximate escape criterion can be seen in [22]). So, the maximum bound value tolerated by our C compiler is $B = 42$ (if we use long double precision) or $B = 35$ (if we use double precision). In this work we shall use a bound of $B = 40$. One might object that escaping past $\operatorname{Re} z = 40$ hardly constitutes escaping to ∞ . However, if $\operatorname{Re} z > 40$, then $\left|\lambda e^{z}\right| > |\lambda| e^{40}$ which is quite large. Moreover, according to Devaney and Durkin [18], the pictures we obtain with this bound are quite accurate.

4.3 *Other Mandelbrot-like sets*

Let us consider now, briefly, the other two Mandelbrot-like sets of families of complex exponential maps that we use in this work. The Mandelbrot-like set of $E_{2\lambda}(z) = e^{z^2+\lambda}$, see Fig. 2, is periodic with period π along the imaginary axis. The period-1 component is unbounded and has infinitely many cusp-like points. Between two of these consecutive cusps, as $\left[-\frac{1}{2}(1+\ln 2)+0i\right]$ and $\left[-\frac{1}{2}(1+\ln 2)+\pi i\right]$, there is a tongue of period-2, two tongues of period-3, and so on, attached to the period-1 component and ordered in a similar manner as the tongues attached to the period-1 cardioid in the BRD set. The tails of the tongues are joined together at the infinity.

In the Mandelbrot-like set of $E_{3\lambda}(z) = e^{z/\lambda}$, see Fig. 3, the tails of the tongues are joined together at the origin and the only unbounded periodic component is the period-1 one.

4.4. *Cantor bouquet*

Let us consider the complement of the BRD set that we call the $\overline{\text{BRD}}$ set. We have

$$\overline{\text{BRD}} = \left\{\lambda \in \mathbf{C} \,\middle|\, E_{1\lambda}^{n}(0) \to \infty \text{ when } n \to \infty\right\}.$$

Let $J(E_{1\lambda})$ be the Julia set of a map of the family $E_{1\lambda}(z) = \lambda e^{z}$. From a proposition of Devaney [15] if $E_{1\lambda}^{n}(0) \to \infty$ then $J(E_{1\lambda}) = \mathbf{C}$, and from a corollary of Devaney [15] there is a Cantor set of curves in the λ -plane for which $J(E_{1\lambda}) = \mathbf{C}$. Then, we can conclude that the $\overline{\text{BRD}}$ set is a Cantor set of curves. We have graphically seen that this result can be extended to the complements of the Mandelbrot-like sets of the families of complex exponential maps of Eqs. (4) and (5): they are Cantor sets of curves.

Given that we use an approximate escape criterion, when we draw the complement of the Mandelbrot-like set of a family of complex exponential maps we cannot see Cantor sets of curves, or "Cantor bouquets" (Devaney and Durkin [18]), but fingers. In the same way, when we draw the Mandelbrot-like set of a family of complex exponential maps we cannot see the small tongues corresponding to higher periods but fingers. In Fig. 4 we can see three representations of a same zone of the BRD set: (a) computer drawing with the approximate escape criterion and bound $B = 10$, (b) computer drawing with the approximate escape

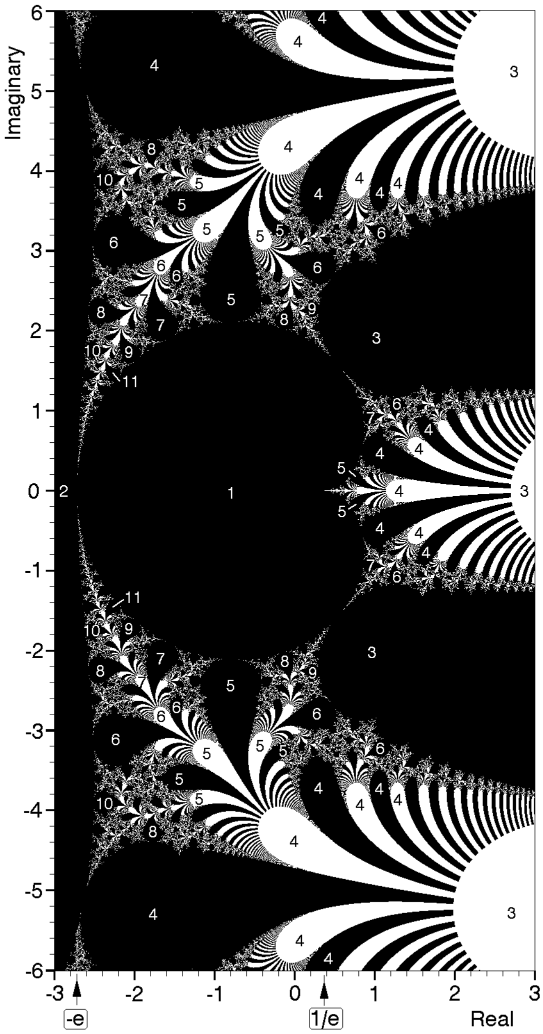

Fig. 1. BRD set or Mandelbrot-like set of $E_{1\lambda}(z)=\lambda e^{z}$.

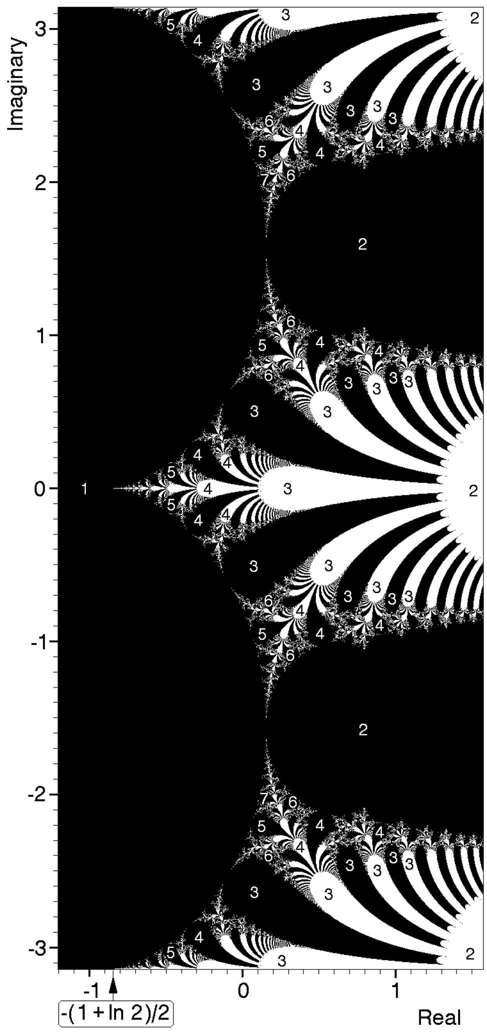

Fig. 2. Mandelbrot-like set of $E_{2\lambda}(z)=e^{z^2+\lambda}$.

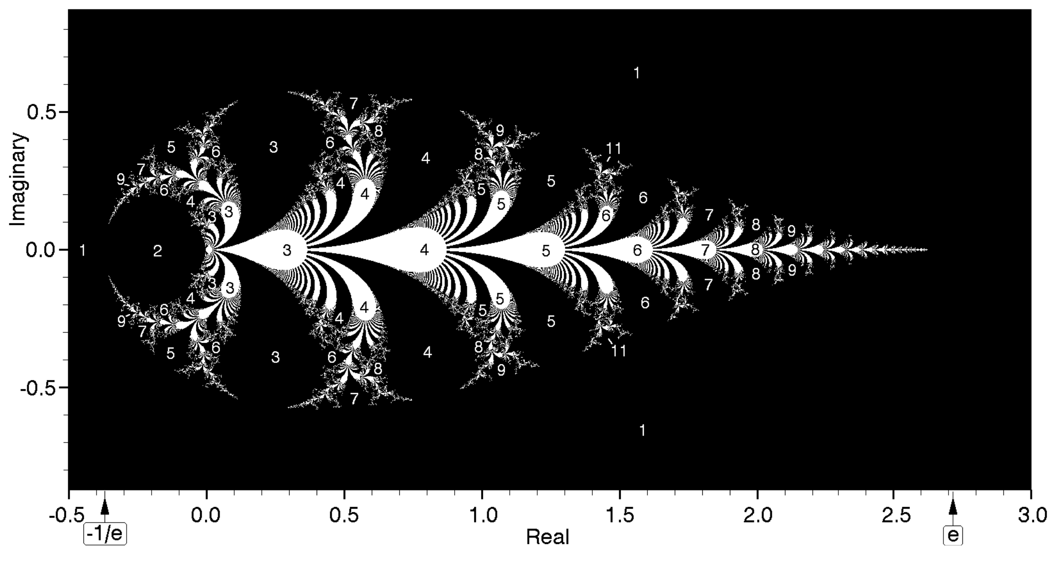

Fig. 3. Mandelbrot-like set of $E_{3\lambda}(z)=e^{z/\lambda}$

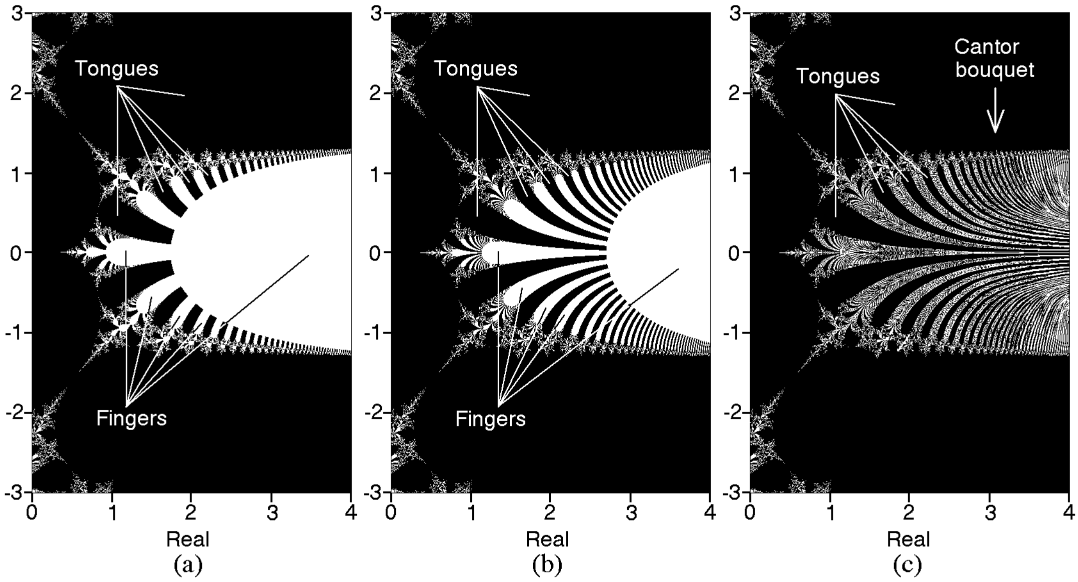

Fig. 4. Tongues, fingers and Cantor bouquet in the BRD set. (a) Computer drawing with the approximate escape criterion $\mathrm{Re}\, z > 10$. (b) Computer drawing with the approximate escape criterion $\mathrm{Re}\, z > 40$. (c) Freehand drawing with a hypothetical $\mathrm{Re}\, z = \infty$ escape criterion.

criterion and bound $B = 40$, and (c) a freehand drawing with a hypothetical exact escape criterion (bound $B = \infty$). In (a) and (b) the fingers impede from seeing completely the tails of the tongues, but the length of each tail that we can see in (b) is greater that in (a). In this figure, black points are bounded and white points escape to ∞. Note that there are points which escape to ∞ in (a) but they do not escape to ∞ in (b): for this reason, (b) is a more precise representation of the BRD set than (a). In (c) the freehand drawing of the BRD set has the fingers missing and the Cantor bouquet appears.

4.5. *Tongues and fingers ordering*

In the Mandelbrot set, the connected set of stable points which give a periodic orbit with the same period is called a hyperbolic component. We have extended this concept to the BRD set, and we have studied the ordering of its tongues C_p of period $p > 2$ [16]. In spite of Baker and Rippon's statement "the distribution of the components C_p, $p > 2$, is extremely complicated" [14], we have shown that the periods of the tongues of the BRD set can be graphically determined with the naked eye by applying two simple rules: the period-adding rule and the counting rule [16].

As we can easily verify graphically in Fig. 2 and Fig. 3, the period-adding rule which we had enunciated in Ref. [16] for the Eq. (3) is also valid in the drawing of the Mandelbrot-like sets of Eqs. (4) and (5). So, "the largest tongue attached to the period-1 component between the period-*n* tongue and the period-*m* tongue (supposing that there is no tongue larger than them in between) has period $n + m$."

Likewise, as we can easily verify graphically in Fig. 2 and Fig. 3, the counting rule which we had enunciated in Ref. [16] for the Eq. (3) is also valid in the drawing of the Mandelbrot-like sets of Eqs. (4) and (5). So, "from each index-*p* finger a bouquet of alternative tongues and fingers, all of them with period $p+1$ or index $p+1$, emerges".

5. JULIA SETS OF EXPONENTIAL MAPS

Let us consider the family of maps of Eq. (3). When λ is a real parameter in the interval $0 < \lambda < 1/e$, the Julia set of the corresponding map of the family is a Cantor set of curves (from a Devaney theorem [15]). On the other hand, when $\lambda = 1 + 0i$ the Julia set is the whole plane (from a Misiurewicz theorem [13]). But, as we can see in the Fig. 1, in the first case the parameter value is inside a black motif of the Mandelbrot-like set of the family of maps, and in the second case the parameter value is inside a white motif of the Mandelbrot-like set of the family of maps.

We have graphically seen that the Julia set of a map of the family of complex exponential maps is a Cantor bouquet if the corresponding parameter value is inside a tongue (or inside the cardioid) of the Mandelbrot-like set of the family, and is the whole plane if the parameter value is inside the complement of this Mandelbrot-like set. In practice the computer drawing of the Julia set is the whole plane if the parameter value is inside a finger of the computer drawing of the Mandelbrot-like set of the family, and the Cantor bouquet is only sketched as a bouquet of tongues and fingers.

5.1. *Horns*

When the parameter value is inside a tongue of the Mandelbrot-like set of a one-parameter family of complex exponential maps, the Julia set of a map of the family has that what we call "horns". Horns were seen

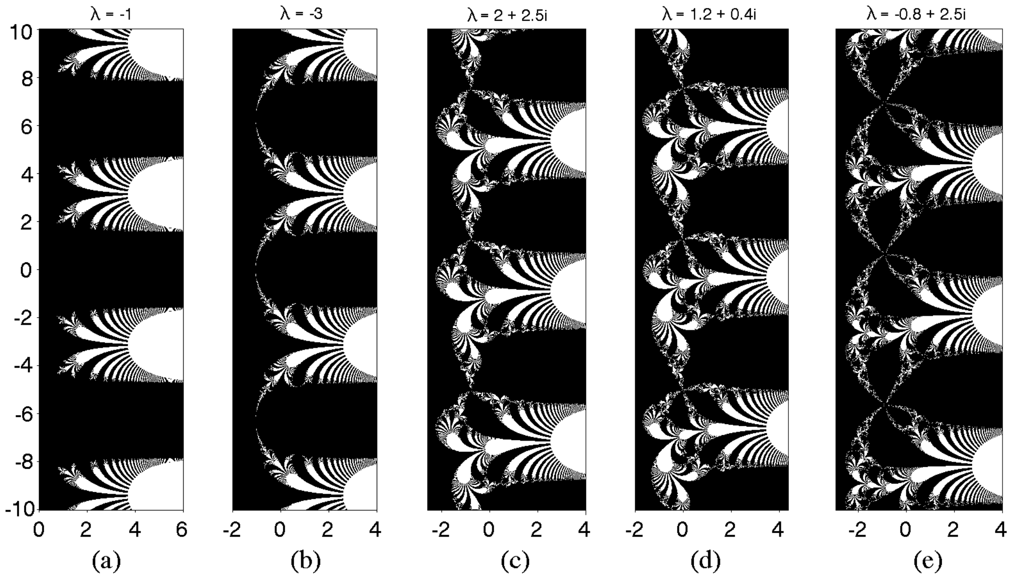

Fig. 5. Horns of the Julia sets of $E_{1\lambda}(z) = \lambda e^z$ for different parameter values. (a) No horn, $\lambda = -1$. (b) Two horns, $\lambda = -3$. (c) Three horns, $\lambda = 2 + 2.5\,i$. (d) Four horns, $\lambda = 1.2 + 0.4\,i$. (e) Five horns, $\lambda = -0.8 + 2.5\,i$.

for the first time by Devaney (see Fig.18.1 of Reference [20]). We have graphically seen that the horns are joined by their tips and they form groups. The number of horns of each group is the same in all the groups of a given Julia set, and it is equal to the period of the tongue ($p > 1$) of the Mandelbrot-like set of the family where the parameter is found.

In Fig. 5 we can see five examples of horns in Julia sets of maps of Eq. (3) for parameter values inside tongues of the BRD set of Fig. 1. In (a) the parameter value of the Julia set is inside the period-1 component bounded by the cardioid; in this case, there is no horn. In (b) the parameter value is clearly inside the period-2 tongue; groups of two horns appears. In (c) the parameter value is inside a period-3 tongue; groups of three horns appears. We can see groups of four and five horns in (d) and (e).

6. GROWTH IN COMPLEX EXPONENTIAL DYNAMICS

6.1. *Misiurewicz points in the BRD set*

As is well known, Misiurewicz points are preperiodic and eventually periodic points. We have studied Misiurewicz points in a family of one-dimensional quadratic maps [23-25], and other authors have studied Misiurewicz points in the Mandelbrot set [7, 8, 9, 26]. In the case of the family of complex exponential maps (3), Misiurewicz points corresponding to imaginary parameter values $\lambda = 2k\pi i$ and $\lambda = (2k+1)\pi i$, $k \in \mathbf{Z}$, have been only recently studied [27]. As we shall see at once, Misiurewicz points corresponding to complex parameter values $\lambda = a + bi$ play an important role in the growth in complex exponential dynamics.

Let $z_{n+1} = f_\lambda(z_n)$ be one of the families (3), (4) or (5). For a given parameter value we have a Misiurewicz point $\mathrm{M}_{n,p}$ if the orbit of $z_0 = 0$ is *n*-preperiodic and *p*-periodic. To calculate the parameter values of the Misiurewicz points $\mathrm{M}_{n,p}$ we have to solve the equation

$$f_\lambda^n(0) = f_\lambda^{n+p}(0) . \tag{7}$$

For example, in the case of the Misiurewicz points $\mathrm{M}_{2,1}$ of the BRD set we have

$$f_\lambda(0) = \lambda ,$$

$$f_\lambda^2(0) = \lambda \exp(\lambda) ,$$

$$f_\lambda^3(0) = \lambda \exp[\lambda \exp(\lambda)] ,$$

and the Eq. (7) gives

$$\exp(\lambda) = \exp[\lambda \exp(\lambda)] . \tag{8}$$

We have to solve Eq. (8). The trivial solution $\lambda = 0$ is not valid, because it corresponds to a parameter value which gives origin to a period-1 orbit (note that a period-1 orbit is also a trivial preperiod-2 and period-1 orbit). We can see that $\lambda = 2k\pi i$, $k \in \mathbf{Z}$, is a trivial solution of Eq. (8) because this parameter value gives $\mathrm{M}_{1,1}$ Misiurewicz points, as we can verify by direct iteration, instead of $\mathrm{M}_{2,1}$ Misiurewicz points. However, $\lambda = (2k+1)\pi i$ is a valid solution of Eq. (8) because this parameter value originates $\mathrm{M}_{2,1}$ Misiurewicz points. Moreover, there is an infinity of $\mathrm{M}_{2,1}$ Misiurewicz points of the form $\lambda = a + bi$. Indeed, if we take into account that $\exp(\lambda) = \exp\,(\lambda + 2k\pi\, i)$, where k is an integer, we have

$$\lambda + 2k_1\pi\, i = \lambda \exp(\lambda + 2k_2\pi\, i) + 2k_3\pi\, i , \tag{9}$$

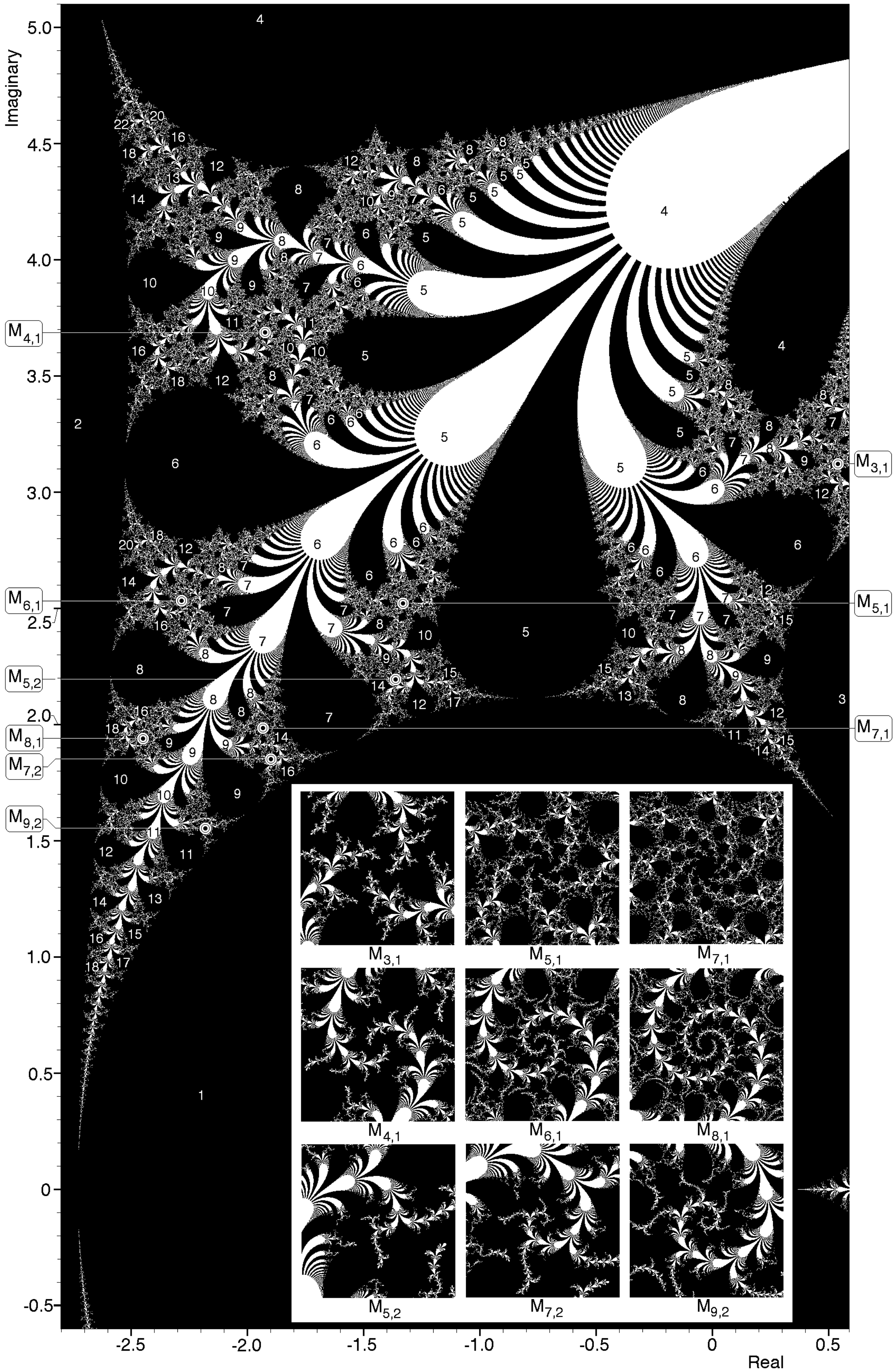

Fig. 6. Misiurewicz points in the BRD set.

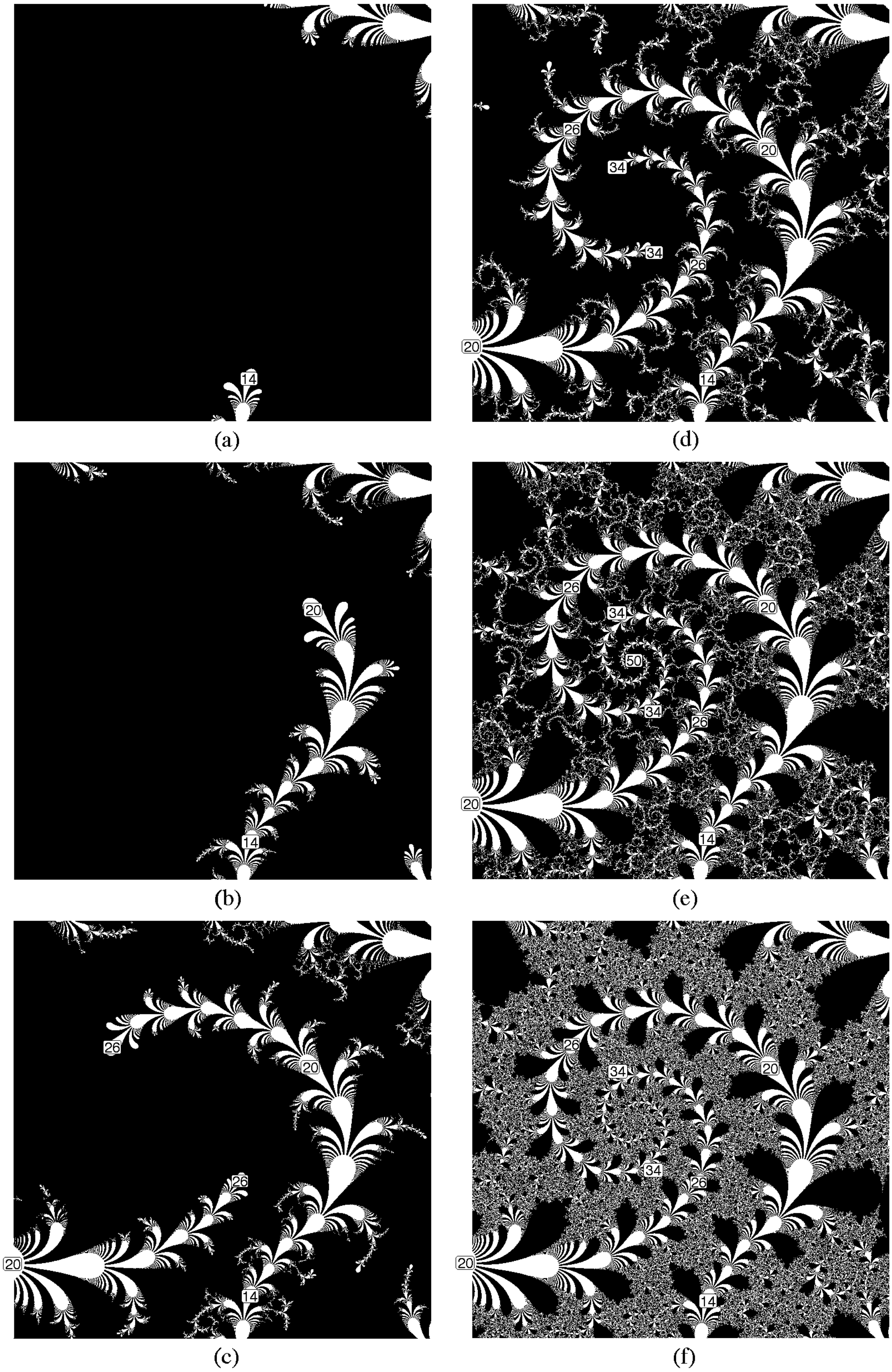

Fig. 7. Growth of the $\overline{\mathrm{BRD}}$ set near the Misiurewicz point $\mathrm{M}_{8,1}$ located at the parameter value $\lambda = -2.437924... + 1.939831...i$. The length of the window square side is 0.111. (a) $N = 14$. (b) $N = 20$. (c) $N = 26$. (d) $N = 34$. (e) $N = 50$. (f) $N = 400$.

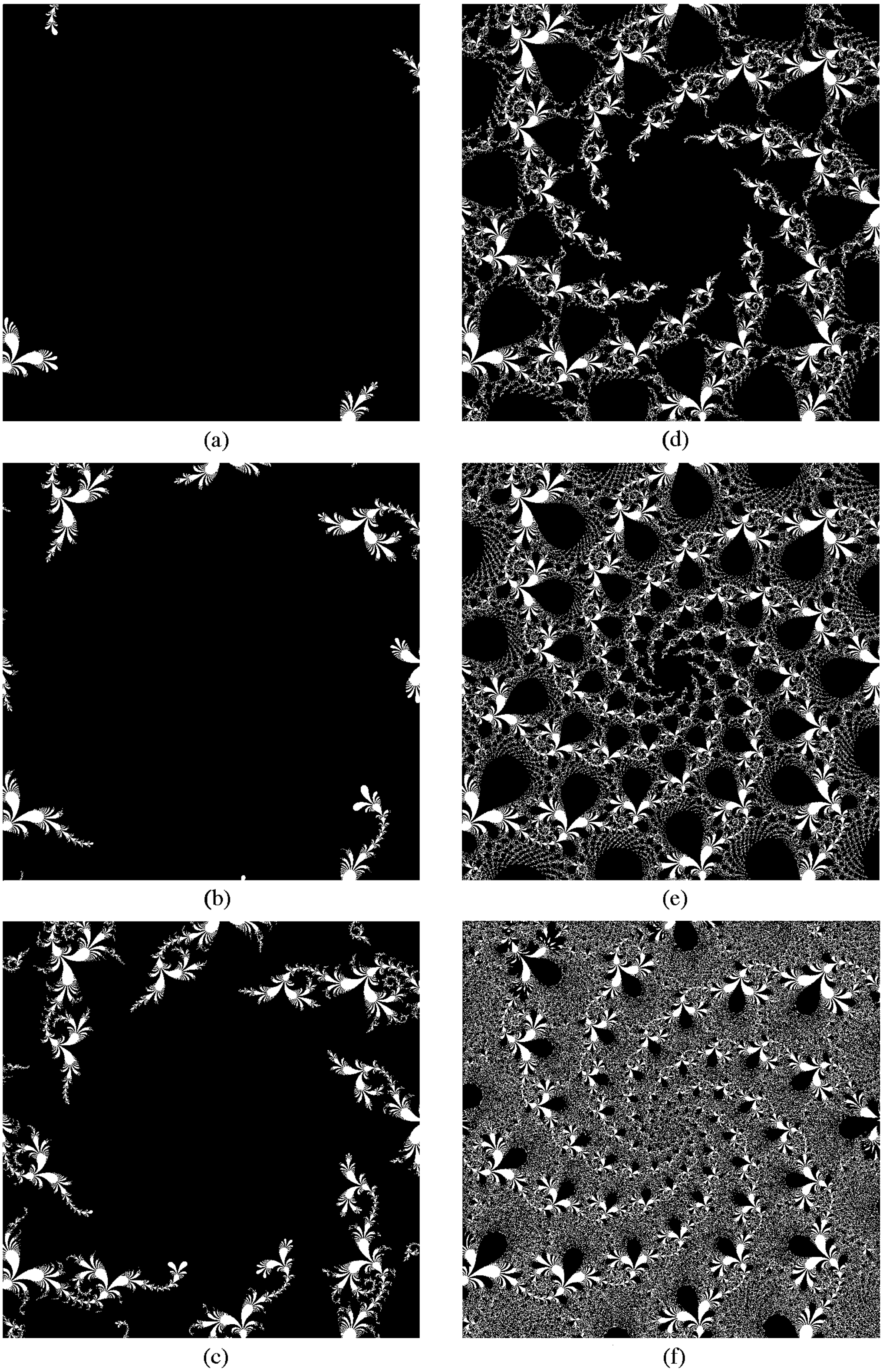

Fig. 8. Growth of the Mandelbrot-like set complement of $E_{2\lambda}(z) = e^{z^2+\lambda}$ near the Misiurewicz point $\mathrm{M}_{9,1}$ located at the parameter value $\lambda = -0.710664070\ldots + 0.021590770\ldots\, i$. The length of the window square side is 4×10^{-6} . (a) N = 225. (b) N = 230. (c) N = 240. (d) N = 260. (e) N = 300. (f) N = 500.

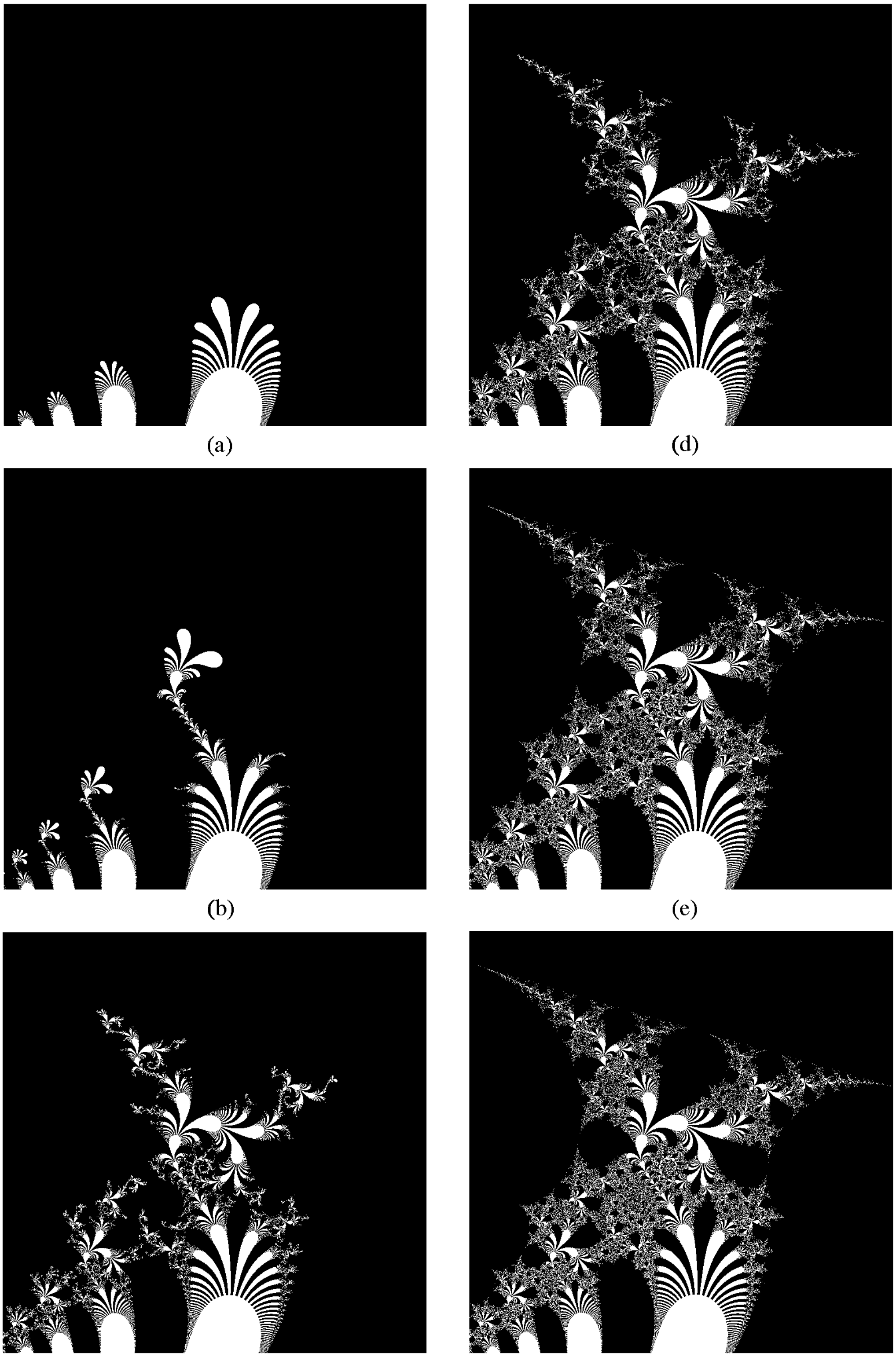

(a) (d)

(b) (e)

(c) (f)

Fig. 9. Growth of the Mandelbrot-like set complement of $E_{3\lambda}(z)=e^{z/\lambda}$. The center of the pictures is the point $2.195+0.08i$ and the length of the window square side is 0.09. (a) N = 12. (b) N = 20. (c) N = 40. (d) N = 80. (e) N = 160. (f) N = 320.

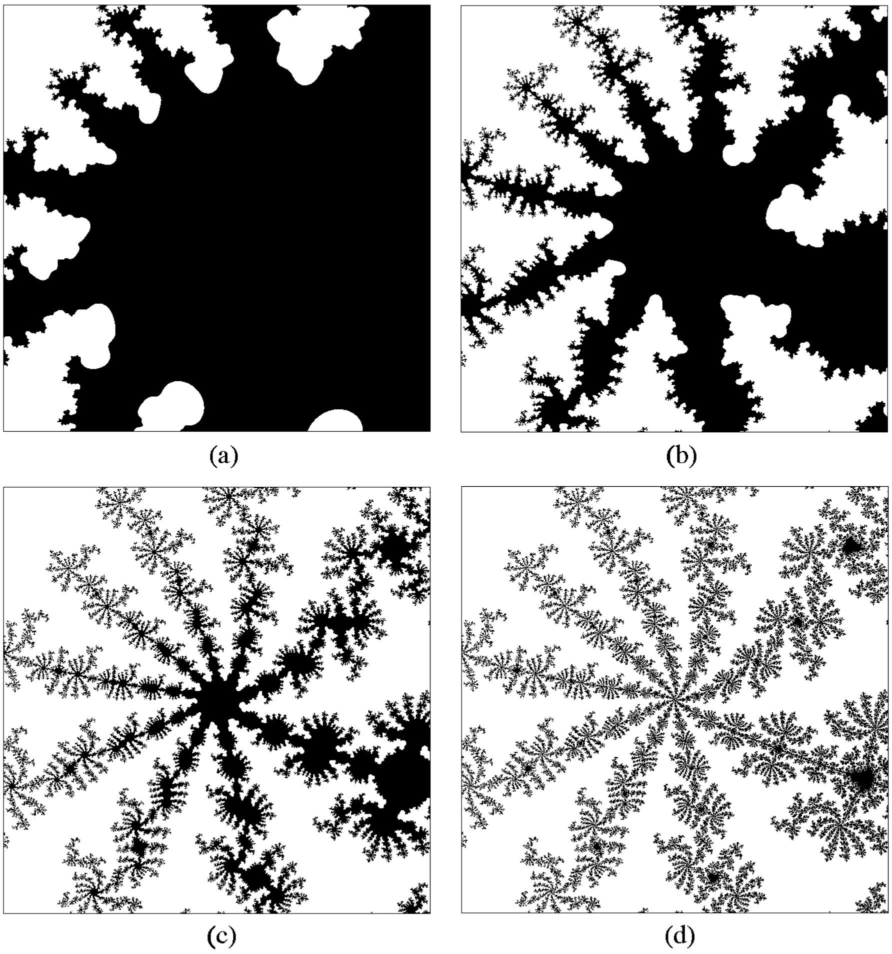

Fig. 10. Computer drawing of the Mandelbrot set near the Misiurewicz point $M_{10,1}$ located at $c = -0.707660\ldots+0.352796\ldots i$. The length of the window square side is 0.022. (a) $N = 35$. (b) $N = 50$. (c) $N = 75$. (d) $N = 300$.

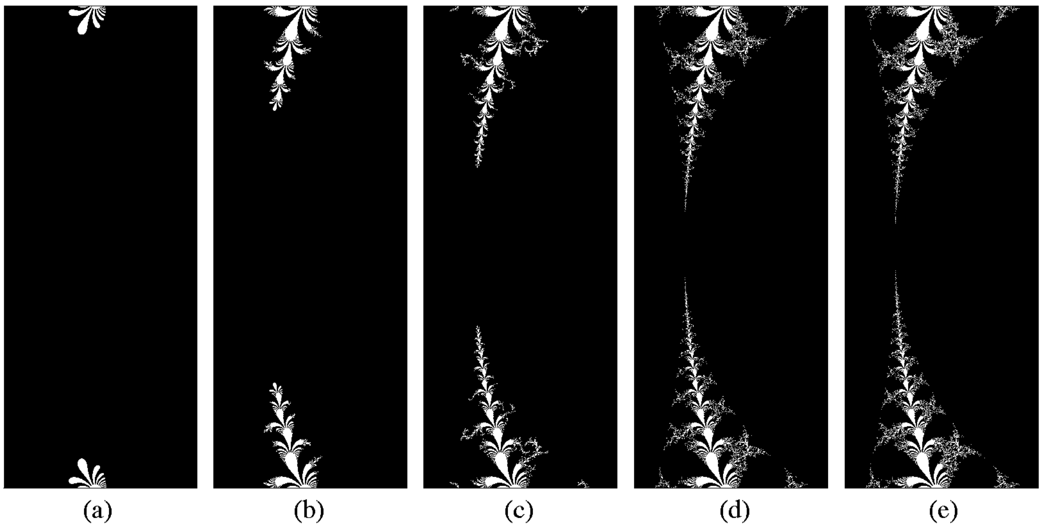

Fig. 11. Growth of the computer drawing of the Mandelbrot-like set complement of $E_{2\lambda}(z) = e^{z^2+\lambda}$ near the multifurcation point located at $\lambda = 0.153\ldots+1.570\ldots\ i$. (a) $N = 8$. (b) $N = 12$. (c) $N = 20$. (d) $N = 50$. (e) $N = 100$.

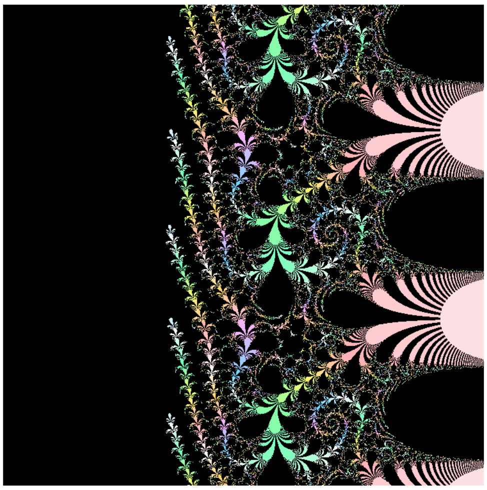

(a) (d)

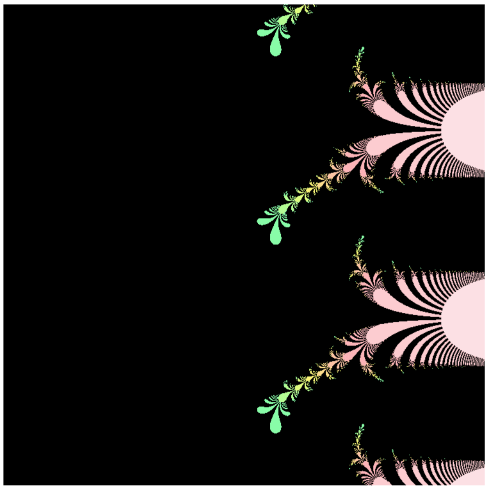

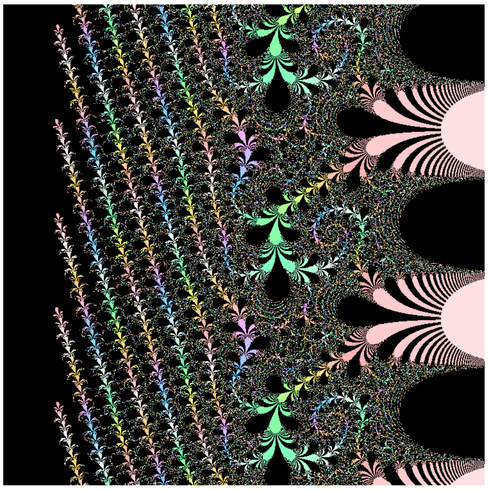

(b) (e)

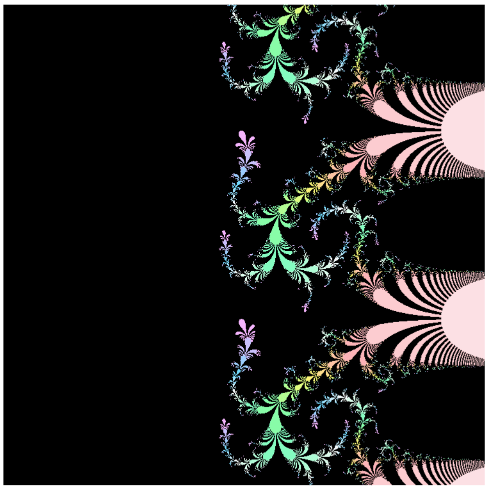

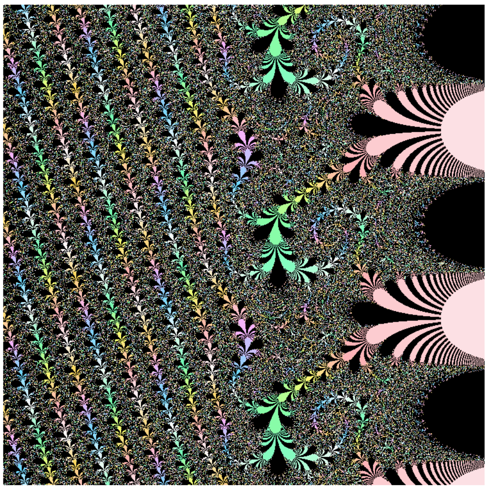

(c) (f)

Fig. 12. Growth of the Julia set of the map $z_{n+1} = (-2.437924 + 1.939831\, i)e^{z_n}$. The center of the pictures is the point $-4+0i$ and the length of the window square side is 16. (a) $N = 5$. (b) $N = 10$. (c) $N = 20$. (d) $N = 40$. (e) $N = 80$. (f) $N = 160$.

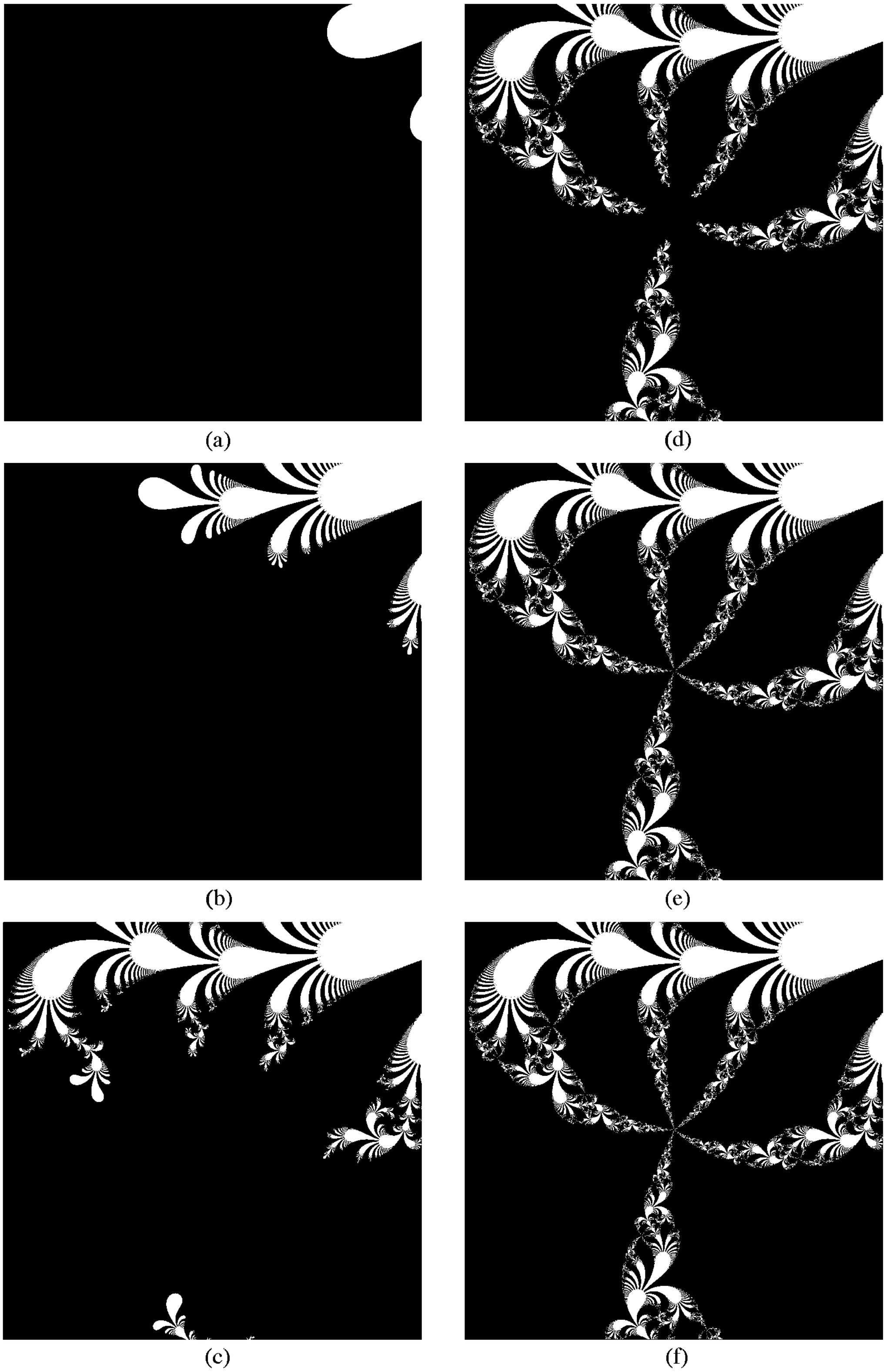

Fig. 13. Growth of the computer drawing of the Julia set of the map $z_{n+1} = e^{z_n/(1.25+0.25i)}$. The center of the pictures is the point $0.693 - 1.24i$, and the length of the window square side is 4.6 . (a) $N = 4$. (b) $N = 6$. (c) $N = 12$. (d) $N = 25$. (e) $N = 50$. (f) $N = 100$.

and for each triad (k_1, k_2, k_3) a different Misiurewicz point $M_{2,1}$ can be obtained. For example, when $k = +1$ and $k_2 = k_3 = 0$ we obtain the Misiurewicz point $M_{2,1}$ located at $\lambda = -1.461204\ldots + 7.127716\ldots\, i$. When $k = -1$ and $k_2 = k_3 = 0$ we obtain the Misiurewicz point $M_{2,1}$ located at $\lambda = 1.461204\ldots -0.844531\ldots i$, and so on. We can verify these results by direct iteration.

We can see some Misiurewicz points in the Mandelbrot-like set of a family of complex exponential maps with the naked eye: they are the centers of very visible spirals. When we have located one of them, we can read its coordinates and later we can obtain its preperiod and period by simple iteration. For example, let us consider the BRD set (see Fig. 6). In this figure we have located nine spirals with the naked eye. The centers of these spirals, that we have marked with concentric circles, are Misiurewicz points. By reading their coordinates and iterating we know they are $M_{3,1}$, $M_{4,1}$, $M_{5,1}$, $M_{6,1}$, $M_{7,1}$, $M_{8,1}$, $M_{5,2}$, $M_{7,2}$, and $M_{9,2}$. In the lower part of the figure, which corresponds to magnifications of the neighborhood of these Misiurewicz points, we can clearly see how the BRD set is in the proximity of each one of these points. We can see, for example, the double spiral around the Misiurewicz point $M_{8,1}$ located at the parameter value $-2.437924\ldots+1.939831\ldots i$.

6.2 *Growth in Mandelbrot-like sets*

In Fig. 7 we can see a six image motion picture of the BRD set near the Misiurewicz point $M_{8,1}$ located at the parameter value $\lambda = -2.437924\ldots+1.939831\ldots i$. The images have been drawn by means of the algorithm of Appendix A using different *N* values. Indexes of representative fingers are shown. We can see that there is a correspondence between the *N* value and the larger finger index in each one of the images. The more accurate drawing of the BRD set corresponds to image (f), when we use an adequate *N* value. Indeed, we clearly can see a lot of cardioid tongues correctly drawn in (f), whereas in (e) and (d) the tongues are not well defined and, finally, in (c), (b) and (a) the tongues are missing.

But these images are rich in ideas, and they evoke a garden in growth. Now, let us consider the complement of the BRD set, the $\overline{\text{BRD}}$ set. According to what has been stated in § 4. 4, the $\overline{\text{BRD}}$ set is a Cantor bouquet which is impossible to see with detail. In Fig. 7 (f) we can visualize, in the proximity of $M_{8,1}$, how this Cantor bouquet is by means of the white fingers. On the other hand, there are a lot of Misiurewicz points surrounding the Misiurewicz point $M_{8,1}$. They are the centers of other spirals that we can clearly see in (e). In the images of Fig. 7, the two main branches of the Cantor bouquet seem to grow around of $M_{8,1}$, and the other branches of the Cantor bouquet seem to grow as well around of other Misiurewicz points. But in the BRD set there are an infinity of Misiurewicz points and therefore this growth is infinitely ramified. We say that the computer drawing of the $\overline{\text{BRD}}$ set, or the computer drawing of the complements of the Mandelbrot-like sets of other families of complex exponential maps, "grow" with *N*. In Fig. 8 we can see another growth example of the computer drawing of the Mandelbrot-like set complement in the case of the family $E_{2\lambda}(z) = e^{z^2+\lambda}$ near the Misiurewicz point $M_{9,1}$ located at the parameter value $\lambda = -0.710664070\ldots +0.021590770\ldots i$. Finally, in Fig. 9 we can see a general view of the growth of the computer drawing of the Mandelbrot-like set complement of the family $E_{3\lambda}(z) = e^{z/\lambda}$.

We think this growth is characteristic of complex exponential dynamics. For example, the family of complex quadratic maps $f(z) = z^2 + c$ behave in a different manner. In Fig. 10 we can see four sketches of the well-known Mandelbrot set in the neighborhood of the Misiurewicz point $M_{10,1}$ located at $c = -0.707660\ldots+0.352796\ldots i$. They are drawn with different *N* values and, as can be seen, there is not a feeling of growth in this case, but a better precision when *N* increases.

The computer drawing of the Mandelbrot-like set complement of a family of complex exponential maps also grow in the proximity of the Mandelbrot-like set nonhyperbolic points where the multiplier is the unity and a multifurcation occurs. For example, let us consider the family $E_{2\lambda}(z) = e^{z^2+\lambda}$. In Fig. 2. we can see a multifurcation point located at the parameter value $\lambda = 0.153\ldots+1.570\ldots\, i$ that corresponds to a bifurcation one (the period of the component on the left is 1 and the period of the tongue on the right is 2). The computer drawing of the Mandelbrot-like set complement grow with the maximal number of iterations towards the multifurcation point, as we can see in Fig. 11.

6.3. *Growth in Julia sets*

We describe here two very different growth kinds in the computer drawings of Julia sets of complex exponential maps. The first one is illustrated in Fig. 12, where we can see a six image motion picture of the computer drawing of the Julia set of $E_{1\lambda}(z) = \lambda e^z$ when $\lambda = -2.437924\ldots+1.939831\ldots i$. This parameter value corresponds to the Misiurewicz point $M_{8,1}$ of the Mandelbrot-like set of the family (see §6.2 and Fig. 6). Each one of these images has been drawn with a different *N* value. As we can see in (d), (e), and (f), there are branches of the Julia set which "grow in a straight line" with *N*. We have verified that this kind of growth also occurs in each one of the nine computer drawings of the Julia sets corresponding to the nine Misiurewicz points depicted in Fig. 6. We can not give now an explanation of this growth, that should be studied in future research.

The second one is illustrated in Fig. 13, where we can see a six image motion picture of the computer drawing of the Julia set of the map of the family

$E_{3\lambda}(z) = e^{z/\lambda}$ that corresponds to the parameter value $\lambda = 1.25 + 0.25\,i$. In Fig. 3 we can easily verify that this parameter value is inside a period-5 tongue of the Mandelbrot-like set of $E_{3\lambda}(z) = e^{z/\lambda}$. According to §5.1 this Julia set shows an infinity of groups of five horns. When *N* is infinite, the horns are exactly joined by their tips. For a finite *N*, the horns grow with *N*.

7. CONCLUSIONS

Both the complement of the Mandelbrot-like set of a family of complex exponential maps and the Julia set of a complex exponential map are Cantor bouquets. But a Cantor bouquet is so thin that we can not see it. In practice, when we draw one of these sets by means of a computer, we use an algorithm with an approximate escape criterion and a finite maximal number of iterations. As a result of all of this, we visualize these sets by means of fingers and tongues instead of a Cantor bouquet. The number of fingers and tongues that we can see grow with the maximal number of iterations in a beautiful manner that evokes the image of a garden in growth. The analysis of this growth around Misiurewicz and multifurcation points helps to us to a better knowledge of the structure of the Cantor bouquet.

ACKNOWLEDGEMENTS

This work was supported by CICYT and SGPICYT (Spain) Research Grants Nos. TEL98-1020 and PB97-1151, respectively.

REFERENCES

1. G. Julia, Mémoires sur l'iteration des fonctions rationnelles, *J. Math. Pure. Appl.* **8**, 47-245 (1918).
2. P. Fatou, Sur les équations fonctionnelles, *Bulletin Société Mathématique de France* **47**, 161-271 (1919); **48**, 33-94 (1920); **48**, 208-314 (1920).
3. R. Devaney, The complex dynamics of quadratic polynomials. In *Complex Dynamical Systems*, R. Devaney (Ed.), American Mathematical Society, Providence, Rhode Island, 1-29 (1994).
4. B.B. Mandelbrot, Fractal aspects of the iteration of $z \to \lambda z(1-z)$ for complex λ and *z*, *Ann. N. Y. Acad. Sci.* **357**, 249-259 (1980).
5. B.B. Mandelbrot, On the quadratic mapping $z \to z^2 - \mu$ for complex μ and *z*; the fractal structure of its *M* set, and scaling, *Physica D* **7**, 224-239 (1983).
6. A. Douady and J.H. Hubbard, Itération des polynômes quadratiques complexes, *C. R. Acad. Sc. Paris* **294**, 123-126 (1982).
7. H.O. Peitgen and P.H. Richter, *The beauty of fractals*, Springer-Verlag, Berlin (1986).
8. B. Branner, The Mandelbrot set. In *Chaos and fractals: the mathematics behind the computer graphics.* Proceedings of Symposia in Applied Mathematics **39**, American Mathematical Society, Providence, 75-105 (1989).
9. J. Milnor, Self-similarity and hairiness in the Mandelbrot set. In *Computers in Geometry and Topology*, Tangora (Ed.), Lecture Notes in Pure and Applied Mathematics **114**, Dekker, New York, 211-257 (1989).
10. A. Douady, Julia sets and the Mandelbrot set. Invited contribution in *The beauty of fractals*, H.O. Peitgen and P.H. Richter, Springer-Verlag, Berlin, 161-173 (1986).
11. B.B. Mandelbrot, *The fractal geometry of nature*, Freeman, San Francisco (1982).
12. M. Romera, G. Pastor, and F. Montoya, Graphic tools to analyse one-dimensional quadratic maps, *Computers and Graphics* **20**, 333-339 (1996).
13. M. Misiurewicz, On iterates of e^z, *Ergod. Theor. Dyn. Syst.* **1**, 103-106 (1981).
14. I.N. Baker and P.J. Rippon, Iteration of exponential functions, *Ann. Acad. Sci. Fenn*. A1 **9**, 49-77 (1984).
15. R. Devaney, Julia sets and bifurcation diagrams for exponential maps, *B. Am. Math. Soc.* **11**, 167-171 (1984).
16. M. Romera, G. Pastor, G. Alvarez, and F. Montoya, Ordering of the Mandelbrot-like set of the exponential map, *Chaos* **8**, 739-740 (1998).
17. R. Devaney, Chaotic bursts in nonlinear dynamical systems, *Science* **235**, 342-345 (1987).
18. R. Devaney and M.B. Durkin, The exploding exponential and other chaotic bursts in complex dynamics, *Am. Math. Mon.* **98**, 217-233 (1991).
19. M. Romera, G. Pastor, G. Alvarez y F. Montoya, Growth in complex exponential dynamics. In *WSCG'98. The Sixth International Conference in Central Europe on Computer Graphics and Visualization'98, Volume II*, V. Skala (Ed.), University of West Bohemia Press, Plzen, Czech republic, 307-314 (1998). URL: http://wscg.zcu.cz.
20. R. Devaney, *A first course in chaotic dynamical systems*, Addison-Wesley, Reading (1992).
21. R. Devaney, Complex dynamics and entire functions. In *Complex Dynamical Systems*, R. Devaney (ed.), American Mathematical Society, Providence, Rhode Island, 181-206 (1994).
22. M.B. Durkin, The accuracy of computer algorithms in dynamical systems, *Int. J. Bifurcation and Chaos* **1**, 625-640 (1991).
23. M. Romera, G. Pastor and F. Montoya, Misiurewicz points in one-dimensional quadratic maps, *Physica A* **232**, 517-535 (1996).
24. G. Pastor, M. Romera and F. Montoya, On the calculation of Misiurewicz patterns in one-dimensional quadratic maps, *Physica A* **232**, 536-553 (1996).
25. M. Romera, G. Pastor and F. Montoya, On the cusp and the tip of a midget in the Mandelbrot set antenna, *Physics Letters A* **221**, 158-162 (1996).
26. J. Stephenson, Spirals in the Mandelbrot set, *Physica A* **205**, 634-664 (1994).
27. R.L. Devaney and X. Jarque, Misiurewicz points for complex exponentials, *Int. J. Bifurcation and Chaos* **7**, 1599-1615 (1997).

APPENDIX A
BRD set

```
/* DATA INPUT
resol    = 768  (example)  Number of image pixels in the 'x' and 'y' direction.
xc, yc   = -3,3 (example)  Cartesian coordinates of the left-up corner of the image.
side     = 6    (example)  Image side length.
iternum  = 25   (example)  Number of iterations. */

/* DRAW THE BRD SET */
inc = side/(resol - 1);
for (iy = 0; iy <= resol - 1; iy++)            /* for each screen line */
{
   icy = yc - iy*inc;                          /* the line ordinate is calculated */
   for (ix = 0; ix <= resol - 1; ix++)         /* for each line pixel */
   {
      icx = xc + ix*inc;                       /* the pixel abscise is calculated */
      x = 0.0; y = 0.0; iter = 0;              /* initial point 0 + 0i */
      do
      {
         ++iter;                               /* next iteration */
         siny = sin(y);                        /* temporary variable */
         cosy = cos(y);                        /* temporary variable */
         expx = exp(x);                        /* temporary variable */
         x = expx*(icx*cosy - icy*siny);       /* the real part is calculated */
         y = expx*(icx*siny + icy*cosy);       /* the imaginary part is calculated */
      } while (iter < iternum  &&  x < 35);
      if (iter == iternum)                     /* if the orbit does not go to ∞ */
         c = 0;                                /* the pixel color is black */
      else                                     /* else */
         c = 15;                               /* the pixel color is white */
      putpixel (ix, iy, c);                    /* the pixel is drawn */
   }
}
```

APPENDIX B
Julia set of map $z_{n+1} = (-2.4290 + 1.9478i)e^{z_n}$

```
/* DATA INPUT
resol   = 768      (example)  Number of image pixels in the 'x' and 'y' direction.
xc, yc  = -12,8    (example)  Cartesian coordinates of the left-up corner of the
image.
side    = 16.0     (example)  Image side length.
iternum = 40       (example)  Number of iterations.
rlambda = -2.4290  (example)  Parameter real part.
ilambda = 1.9478   (example)  Parameter imaginary part. */

/* DRAW THE JULIA SET */
inc = side/(resol - 1);
for (iy = 0; iy <= resol - 1; iy++)            /* for each screen line */
{
   y0 = yc - iy*inc;                           /* the line ordinate is calculated */
   for (ix = 0; ix <= resol - 1; ix++)         /* for each line pixel */
   {
      x = xc + ix*inc;                         /* the pixel abscise is calculated */
      y = y0; iter = 0;                        /* initialize line ordinate */
      do
      {
         ++iter;                               /* next iteration */
         siny = sin(y);                        /* temporary variable */
         cosy = cos(y);                        /* temporary variable */
         expx = exp(x);                        /* temporary variable */
         x = expx*(rlambda*cosy - ilanda*siny);/* the real part is calculated */
         y = expx*(rlambda*siny + ilanda*cosy);/* the imaginary part is calculated */
      } while (iter < iternum  &&  x < 35);
      if (iter == iternum)                     /* if the orbit does not go to ∞ */
         c = 0;                                /* the pixel color is black */
      else                                     /* else */
         c = 15;                               /* the pixel color is white */
      putpixel (ix, iy, c);                    /* the pixel is drawn */
   }
}
```